

Determination of the spin torque non-adiabaticity in perpendicularly magnetized nanowires

J. Heinen,¹ D. Hinzke,¹ O. Boulle,² G. Malinowski,³ H. J. M. Swagten,⁴ B. Koopmans,⁴ C. Ulysse,⁵ G. Faini,⁵ and M. Kläui^{6,7, a)}

¹⁾*Fachbereich Physik, Universität Konstanz, 78457 Konstanz, Germany*

²⁾*Spintec, UMR CEA / CNRS / UJF-Grenoble 1 / Grenoble-INP, 38054 Grenoble Cedex 9, France*

³⁾*Laboratoire de physique des solides, Université Paris-sud, 91405 Orsay, France*

⁴⁾*Department of Applied Physics, Eindhoven University of Technology, 5600 MB, The Netherlands*

⁵⁾*CNRS, Phynano team, Laboratoire de Photonique et de Nanostructures, 91460 Marcoussis, France*

⁶⁾*SwissFEL, Paul Scherrer Institut, 5232 Villigen PSI, Switzerland and Laboratory for Nanomagnetism and Spin Dynamics, Ecole Polytechnique Fédérale de Lausanne (EPFL), 1015 Lausanne, Switzerland*

⁷⁾*Institut für Physik, Johannes Gutenberg-Universität, 55099 Mainz, Germany*

(Dated: 19 October 2011)

Novel nano-fabrication methods and the discovery of an efficient manipulation of local magnetization based on spin polarized currents has generated a tremendous interest in the field of spintronics. The search for materials allowing for fast domain wall dynamics requires fundamental research into the effects involved (Oersted fields, adiabatic and non-adiabatic spin torque, Joule heating) and possibilities for a quantitative comparison. Theoretical descriptions reveal a material and geometry dependence of the non-adiabaticity factor β , which governs the domain wall velocity. Here, we present two independent approaches to determine β : (i) Measure the dependence of the dwell times for which a domain wall stays in a metastable pinning state on the injected current and (ii) the current-field equivalence approach. The comparison of the deduced β values highlights the problems using 1D-models to describe 2D-dynamics and allows us to ascertain the reliability, robustness and limits of the used approaches.

^{a)}Mathias.Klaeui@magnetism.ch

Also at Fachbereich Physik, Universität Konstanz, 78457 Konstanz, Germany.

I. INTRODUCTION

The probably best known data storage device is the magnetic hard disk,¹ which during the last years has started to face stiff competition from novel memory concepts.²⁻⁵ Flash memory, MRAM and the racetrack memory are based on the usage of electric currents and charges to store and control informations. The latter two are based on magnetic materials and therefore potentially share the advantage of virtually unlimited endurance and good data retention with the magnetic hard disk. Furthermore, their advantages over hard drives are fast access times and the fact, that they work without mechanically moving parts, which are energy-consuming.

Despite the new approaches to manipulate the magnetization, the interpretation of information (bits 0 and 1) as magnetic domains pointing in a left/right (up/down) direction remains. So called domain walls (DWs) separate the domains from each other and the size of the domain and the DW width are thus limiting the data storage density. Various effects can be used to manipulate magnetic domains and the DWs delineating them. In case of magnetic disk drives, a read/write head is moved mechanically across a magnetic material and allows for a local manipulation of the domains using an external field. Nowadays, novel nano-fabrication methods open a new path to encode information within a simple nanowire structure on a few hundred nanometer scale. Here, localized injection of current is used to manipulate the magnetization using various effects. The most obvious effect is the creation of an Oersted field, which is commonly used to create DWs. The more exciting effect is the interaction of a spin polarized current with the local magnetization, especially the influence on the DW dynamics. This interaction is mainly characterized by two torques: i) the adiabatic torque and ii) the non-adiabatic torque, which is caused by several mechanisms. In experiments it was found that these effects are strongly dependent on the materials used and the magnetization configuration (in-plane or out-of-plane). Introducing the non-adiabaticity factor β , which governs the DW velocities, allows for the comparison between the experiments. Nevertheless, a wide variety of values has been found highlighting the problems in separating the mentioned effects and their quantitative description.

In this paper, we focus on approaches to determine the contribution of the Oersted field effect and spin torque to the current induced domain wall dynamics. Two experimental approaches are being presented, which we use to deduce the spin torque non-adiabaticity β

and we discuss their reliability considering the 2D nature of the DWs when using 1D-models.

II. THEORY OF TORQUES ACTING ON DOMAIN WALLS

A. Field induced domain wall motion (Oersted field effects)

The most obvious effect to manipulate magnetic domains is an externally applied magnetic field, which can drive a single domain wall, but will move two adjacent domain walls in opposite directions. In addition to the spin torque effects described below, a charge current, which is flowing in a non-magnetic or magnetic material, is also creating a local Oersted field according to the Biot-Savart law. This Oersted field can create and move a DW.⁶⁻¹⁰ On the nanoscale, disadvantages of this approach arise, because high current densities are needed to create the necessary large magnetic fields and this entails disadvantageous scaling. However, in this work we focus only on currents flowing in a magnetic wire that also contains the domain walls and so we do not deal with the Oersted field created externally in separate structures. But a current flowing through a magnetic nanowire also creates an Oersted field. Simulations of a perfect nanowire show that the net force on a DW should be zero, but in out-of-plane magnetized materials it can lead to local depinning of the DW at the edges of the wire, where an effective local Oersted field is present. In soft-magnetic materials with a perpendicular uniaxial anisotropy it might also lead to a complete change of the domain structure e.g. change into a DW aligned along the wire, which then can be reversibly switched due to the Oersted field.¹¹

B. Adiabatic torque

Another approach to manipulate locally the magnetization within nanostructured devices was first introduced by Berger more than 30 years ago.¹² This approach is based on the interaction of spin polarized conduction electrons with the local magnetization. When crossing a sufficiently wide DW, the conduction electron spins can adiabatically follow the local magnetization transferring angular momentum due to the conservation of total spin and thus driving a domain wall along the electron flow direction.¹³⁻¹⁵ The wall velocity u resulting from this angular momentum transfer can be calculated as follows: $u = JPg\mu_B/2eM_s$ with the Bohr magneton μ_B , the current spin polarization P and the saturation magnetization

M_s .^{13,14}

C. Non-adiabatic torque

In case of a narrow DW, non-adiabatic effects can occur, which are first introduced by Zhang et al.¹⁵ and Thiaville et al.¹⁶ describing spin relaxation processes (SR)¹⁴⁻¹⁷ and a linear momentum transfer (NA)^{13,14,18-20}. These effects can significantly alter the DW dynamics regarding DW velocity and critical current density. Introducing a dimensionless non-adiabaticity factor $\beta = \beta_{\text{SR}} + \beta_{\text{NA}}$ including both non-adiabatic contributions, the final velocity now scales below the Walker breakdown as follows: $v = \frac{\beta}{\alpha}u$ with the Gilbert damping constant α .^{15,17,21} Therefore, the search for materials with a large non-adiabaticity factor β is a focus of spintronic research.

D. Description using 1D-model with and without thermal excitation

Using a set of two parameters (DW center position q , effective out-of-plane angle Ψ) it is possible to describe the DW dynamics for a rigid domain wall profile:¹⁶

$$\dot{\Psi} + \frac{\alpha \dot{q}}{\lambda} = \gamma \mu_0 H + \frac{\beta u}{\lambda} - \frac{\gamma}{2M_s} \frac{\delta V_{\text{pin}}}{\delta q} \quad (1)$$

$$\frac{\dot{q}}{\lambda} - \alpha \dot{\Psi} = \frac{\gamma \mu_0 H_k}{2} \sin 2\Psi + \frac{u}{\lambda} \quad (2)$$

with the gyromagnetic ratio $\gamma = g\mu_B/\hbar$, the restoring field for the transverse orientation H_k , the applied perpendicular external magnetic field H , the DW velocity $u = JPg\mu_B/2eM_s$ and the pinning potential $V_{\text{pin}}(q, \Psi)$. The domain wall width is defined as: $\lambda = \sqrt{\frac{A_{\text{ex}}}{K_0 + K\sin^2\Psi}}$ with the exchange constant A_{ex} , the uniaxial longitudinal anisotropy K_0 and the transverse anisotropy K .²² In the pure adiabatic case ($\beta = 0$) a critical current density J_c is necessary to drive a DW with the velocity $u_c = \gamma\mu_0 H_k \lambda/2$, which is derived by finding the stationary solutions of Eq. 1 and 2.^{17,21}

In most experiments the critical current density exceeds 1×10^{12} A/m² leading to significant Joule heating effects, which are not taken into account so far in this 0 K model.

The 1D-model described above can be extended by adding stochastic Gaussian distributed forces η_Ψ and η_q to account for thermal effects, which has been introduced by Duine et al.²³.

Following his approach, one can rewrite the equations of motion as:

$$\dot{\Psi} + \frac{\alpha \dot{q}}{\lambda} = -\frac{\gamma}{2M_S} \frac{\delta V_{\text{eff}}}{\delta q} + \eta_{\Psi} \quad (3)$$

$$\frac{\dot{q}}{\lambda} - \alpha \dot{\Psi} = -\frac{\gamma}{2M_S \lambda} \frac{\delta V_{\text{eff}}}{\delta \Psi} + \eta_q \quad (4)$$

including an effective potential, which summarizes the terms for the adiabatic and non-adiabatic torques, the external field H , the demagnetizing field H_K and the pinning potential $V_{\text{pin}}(q, \Psi)$:

$$V_{\text{eff}} = \mu_0 H_K M_S \lambda \sin^2 \Psi + \frac{2M_S}{\gamma} u \Psi - 2M_S q \left(\mu_0 H + \frac{\beta u}{\lambda \gamma} \right) + V_{\text{pin}}(q, \Psi) \quad (5)$$

Associated with V_{eff} one can now calculate the energy barrier ϵ , which a DW has to overcome.

E. Extracting the non-adiabatic spin torque (β)

One of the key challenges in the field of current-induced domain wall motion is to determine to what extent the adiabatic torque, the non-adiabatic torque or the Oersted field contribute to the wall displacement. The most important question to understand the spin torque effect including the efficiency of the non-adiabatic torque and thus the value of β . Two independent approaches to extract the non-adiabaticity have been put forward: i) the current-field equivalence and ii) the measurement of the influence of current on the motion of a domain wall across an energy barrier, which a DW has to overcome before DW displacement occurs.

1. Current-field equivalence

The first approach can directly be deduced from the equations of motion of the 1D-model. From Eq. 1 and 2 it can be seen that the non-adiabatic torque enters as an effective field $\mu_0 H_{\text{eff}} = \beta u / \gamma \lambda = \epsilon J$ with the efficiency $\epsilon = \beta P \hbar \pi / (2e M_S \lambda)$.^{24,25} The efficiency can now be determined by studying the interaction of applied fields and injected currents e.g. during DW depinning processes. This current-field equivalence is also independent of the concrete spin structure.

2. Arrhenius law approach

The second approach is based on the assumption that a rigid and simple DW can be described as a quasi particle moving in a 1D-potential landscape. Here, we consider the case of a DW hopping between two metastable states, where the thermally activated motion from one energy potential well to another can be described by the Arrhenius law.²⁶ The dwell time τ_S for which a DW stays in one state S is an exponential function of the current dependent energy barrier $\epsilon(J)$:^{26,27}

$$\frac{1}{\tau_S} = \frac{1}{\tau_{0,S}} e^{-\frac{\epsilon(J)}{k_B T}} \quad (6)$$

and therefore a strong influence from even small current densities J is expected. For the current dependent shift in energy, Eltschka et al.²⁸ derived the following expression:

$$\epsilon_J = \frac{2\beta A \hbar P X_0}{e} \frac{J}{\lambda} \quad (7)$$

with the electron charge e, DW cross-sectional area A, spin polarization P, hopping distance X_0 and the domain wall width λ . By determining the dwell times for which a domain remains in a state, one can use the following equation

$$\ln\left(\frac{\tau_1}{\tau_0}\right) = \ln\left(\frac{\tau_{0,1}}{\tau_{0,0}}\right) + \frac{\epsilon_{0,1} - \epsilon_{0,0}}{k_B T} + \sigma J \quad (8)$$

with $\sigma = \frac{2A\hbar\beta P X_0}{k_B T e \lambda}$ to calculate the non-adiabaticity β .

F. Joule heating effects

Another effect, which occurs when injecting high current densities into nanowires, is Joule heating. This effect may lead to local temperature increases up to a few hundred Kelvin^{24,29} depending on the wire structure, material composition and the possibility of heat dissipation^{30,31} into the surrounding environment and therefore alters the experimental settings. E.g. in depinning field experiments, thermal energy helps the DW to overcome the pinning barrier and thus affects the necessary torque, which is the focus of most studies.

III. EXPERIMENTS

To tailor materials that exhibit fast domain wall motion resulting from large non-adiabatic effects one wants to enhance the non-adiabaticity and this is expected to occur for strong

magnetization gradients, which are present in out-of-plane magnetized materials. These materials are characterized by a strong uniaxial anisotropy pointing out of the film plane, which is defined as $K_{\text{eff}} = K - \mu_0 M_S^2/2$ with the transverse anisotropy K and the shape anisotropy. In out-of-plane magnetized nanowires two domain wall types are possible:^{22,32,33} (i) the Bloch wall, where the current is always flowing perpendicular to the local magnetization, or the (ii) Néel wall type, which is stable in case of e.g. Co/Ni nanowires with widths below 100 nm.⁹ Both DW types and their dynamics can be described as a first approximation using the 1D-model. The theoretical approaches described above are also suitable to describe the experimental results and especially to extract the spin torque non-adiabaticity. Therefore, nanowires with a strong perpendicular anisotropy using a Pt(2 nm)/[Co(0.6 nm)/Pt(1.4 nm)]₂/Co(0.6 nm)/Pt(2 nm) multilayer material and attached Hall crosses have been fabricated on a Si/SiO₂(220 nm) substrate by sputtering (see Fig. 1a). The effective easy-axis magnetic anisotropy $K_{\text{eff}} = 2.7 \times 10^5 \text{ J/m}^3$ (at 300 K) and the saturation magnetization $M_S = 1.4 \times 10^6 \text{ A/m}$ were determined previously.²⁴ Assuming an exchange constant $A_{\text{ex}} = 1.6 \times 10^{-11} \text{ J/m}$,³⁴ allows us to estimate the DW width $\lambda = \sqrt{\frac{A_{\text{ex}}}{K_{\text{eff}}}} \approx 6.3 \text{ nm}$ in our wires, which is much smaller than in in-plane magnetized materials with comparable wire geometries.^{28,35}

Nanowire structures using Cu(6 nm)/[Ni(0.6 nm)/Co(0.2 nm)]₅ as a multilayer material are fabricated as well. Extraordinary Hall measurements using an external field perpendicular to the wire plane reveal square hysteresis loops. The material parameters of similar Co/Ni multilayer materials have been measured by several groups:^{7,9,29} saturation magnetization $M_S \approx 6.6 \times 10^5 \text{ A/m}$ and $K_{\text{eff}} \approx 4.1 \times 10^5 \text{ J/m}^3$. Assuming again an exchange constant $A_{\text{ex}} = 1.6 \times 10^{-11} \text{ J/m}$ one finds a DW width $\lambda \approx 6.2 \text{ nm}$.

A. Separating the acting torques

For all of the described effects, one can find the following symmetries considering the configuration of the local magnetization and the polarity of the injected current:

1. Joule heating effect: This effect is independent of the magnetization configuration and the polarity of the injected current leading in most cases to a reduction of a pinning potential and therefore reduces the necessary depinning field of a DW with increasing current and thus heating.

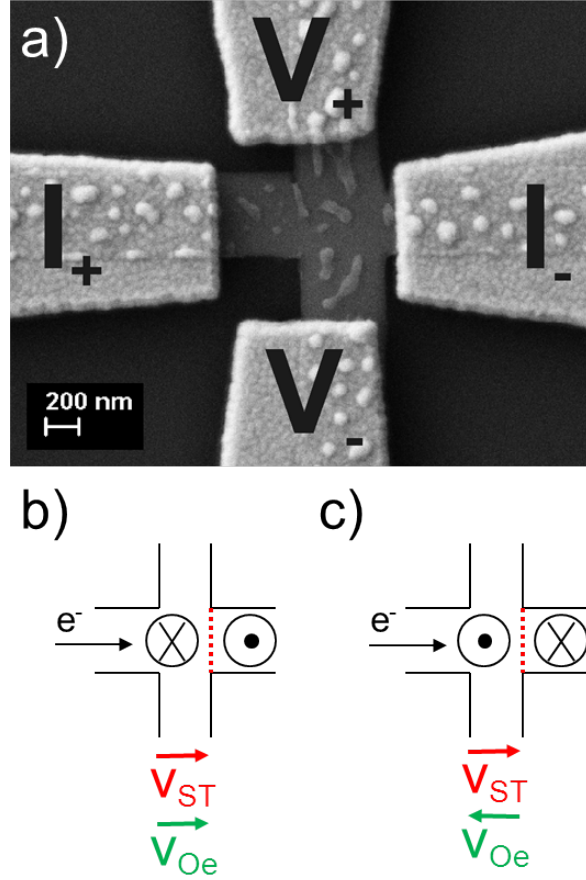


FIG. 1. a) Scanning electron microscopy image of the Hall cross geometry [Pt(2 nm)/[Co(0.6 nm)/Pt(1.4 nm)]₂/Co(0.6 nm)/Pt(2 nm)] used to detect and pin DWs. The current (I) and voltage (V) contacts are indicated. Remaining resist from the lift-off process can be seen. Injection of current along the wire leads to the creation of a concentric Oersted field and a spin torque. The spin torque will move the DW with a velocity (V_{ST}) to the right independent of the magnetization configuration along the electron flow direction. In contrast, the created Oersted field will move the DW in the same direction as the current in case b), whilst it will move it in the opposite direction in case c) indicated by DW velocities (V_{Oe}) of opposite direction.

- Oersted field effect: Depending on both parameters, polarization of current and local magnetization, this effect will be inverse, when the current polarity (I_+ or I_-) or the magnetisation in the domain (M_+ or M_-) is reversed (see Fig. 1b and 1c): $H_{Oe}(I_+, M_+) = -H_{Oe}(I_+, M_-)$ and $H_{Oe}(I_+, M_+) = -H_{Oe}(I_-, M_+)$

3. Spin torque: The adiabatic and non-adiabatic contributions only depend on the current polarity and are independent of the initial magnetization configuration. This can be expressed as (see Fig. 1b and 1c): $H_{\text{ST}}(I_-, M_+) = H_{\text{ST}}(I_-, M_-) = -H_{\text{ST}}(I_+, M_+) = -H_{\text{ST}}(I_+, M_-)$

The depinning field under the influence of current can therefore be expressed as follows:

$$H_{\text{dep}} = H_{\text{ST}} + H_{\text{Oe}} + H_{\text{Joule}}.^{36}$$

B. Experimental results: Domain wall depinning in Co/Pt multilayer wires

Various experiments focus only on a single magnetization configuration in order to study the influence of current on the depinning field of a DW. With this, most of the experiments have not been able to clearly separate the contribution of each torque unambiguously. In case of the out-of-plane materials, recent measurements revealed large β values (larger than α and even larger than in permalloy).^{13,24,28,29,37-43} This used approach is valid as we can show that a weak pinning regime Ib as defined in Ref. 17, where β governs the depinning, is present. A weak pinning regime Ia, where the adiabatic torque (the so called spin transfer in Ref. 17) matters, can be excluded since the critical current density j_c^{1a} is much larger than the maximum current density used in our experiments. Furthermore, we can exclude the intermediate pinning regime since no constant threshold current density for DW motion, which is predicted in Ref. 17, is present in the results shown below. Last, we exclude the strong pinning regime, where no DW motion would occur. An example for the strong pinning regime is presented by Bisig et al. studying tunable steady-state DW oscillators.⁴⁴

Taking into account the symmetries of all the mentioned effects and resulting torques, we have studied the variation of the depinning field as a function of injected current density to separate the contributions and extract the spin torque non-adiabaticity.³⁶ We first reproducibly place a DW at the entrance of a Hall cross with both possible initial magnetization configurations (see Fig. 2a). We then start at zero field, where the extraordinary Hall voltage indicates that the DW is being reproducibly pinned at the same position. Performing the experiment at a low cryostat temperature reduces the possibility of a thermally activated DW depinning process. Under the influence of injected current pulses, we observe a decrease of the depinning field with increasing current density and an obvious splitting between both current polarities (see Fig. 2b). The overall decrease can be attributed to Joule heating, whilst the splitting can be either due to Oersted field effects or spin torque effects. The

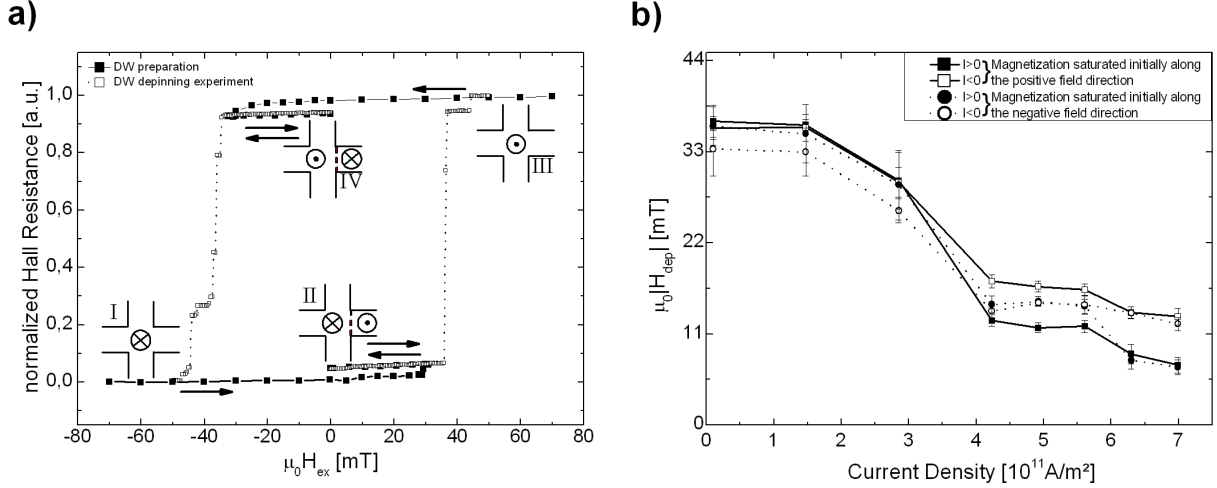


FIG. 2. a) Normalized Hall resistance as a function of the applied perpendicular external field at a constant cryostat temperature $T_{Cryo} = 100 K$. The filled square, solid line curves correspond to the preparation of the DWs, while each point of the open square, dotted line curves is measured after the injection of a single pulse with a current density of $J = 1.02 \times 10^{10} A/m^2$. b) $|H_{dep}|$ as a function of the injected current density for both initial magnetization configurations. The measurement points represent the mean values of $|H_{dep}|$ averaged over at least 8 repetitions, whilst the error bars show the standard deviation. [From Ref. 36]

combination of four measurements (I_{\pm}, M_{\pm}) allows us to deduce each contribution to the depinning field using the mentioned symmetries (for details see Ref. 36). The result shows almost zero Oersted field contribution and a non-zero spin torque contribution (see Fig. 3). Concerning the adiabatic torque, the calculated critical current density J_c is much higher than the injected current densities used in the experiment and therefore does not contribute to the DW depinning.

1. Current-field equivalence

A quantitative description of the spin torque is given by the non-adiabaticity factor. Here, we used the current-field equivalence mentioned above. Analyzing the efficiency $\epsilon = \beta P \hbar \pi / (2e M_S \lambda)$, which is defined as the slope $|\mu_0 \Delta H_{dep} / \Delta J|$, allows us to directly deduce the non-adiabaticity factor β . The material parameters used are: current spin polarization $P = 0.46$ (assumed to be similar to the one of pure Co), domain wall width $\lambda = 6.3$ nm and

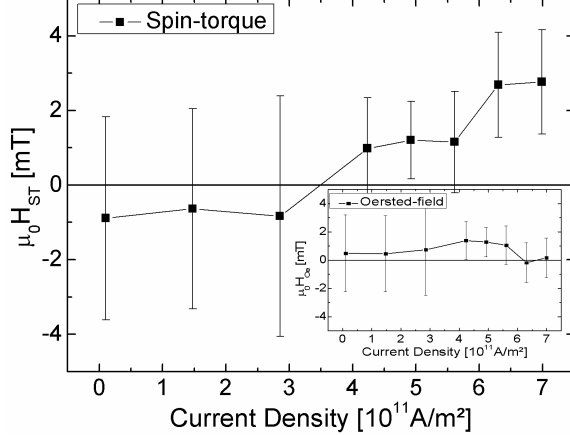


FIG. 3. From the deduced contributions for spin torque and for Oersted field (inset), we can extract the efficiency ϵ using a linear fit through the origin (zero spin torque for zero current density) and including the points with the lowest Oersted field contribution. [From Ref. 36]

saturation magnetization $M_S = 1.4 \times 10^6$ A/m. The Joule heating has been extracted during the calculations, but one has to consider that the sample temperature was changing during the pulse injection. Complementary experiments of Boule et al.²⁴ allow us to approximate the sample temperature increase during the pulse injection. We find that the sample temperature increases for the highest injected current densities up to 300 K, when starting at a constant cryostat temperature of 100 K thus allowing us to compare the derived β values. It turns out that the derived $\beta = 0.24$ is of the same order of magnitude compared to the derived value $\beta = 0.35$ by Boule et al.²⁴ at a constant sample temperature (300 K) and almost double the Gilbert damping constant $\alpha \approx 0.15$.⁴⁵

C. Experimental results: Dominant adiabatic spin torque in Co/Ni multilayer wires

The knowledge gained from the Co/Pt experiment (see sec. III.B) allows us to extend these experiments to the Co/Ni multilayer material. Using a short wire structure ($< 2\mu m$) with attached Hall crosses, which are in close proximity to each other, we are able to inject short 10 ns long pulses to reduce Joule heating effects. Following the depinning field measurement scheme used before on the Co/Pt multilayer wires,³⁶ we are able to separate the spin torque and Oersted field contribution at a constant cryostat temperature of 200 K.

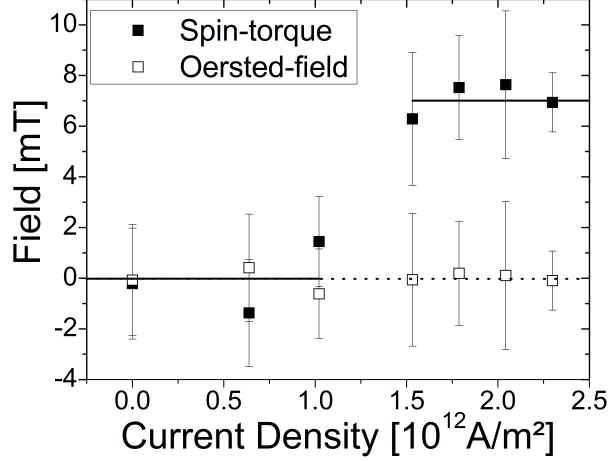


FIG. 4. The spin torque and Oersted field contribution are being deduced by following the measurement scheme used for the Co/Pt multilayers.³⁶ At a current density of 1.5×10^{12} A/m 2 a step in the spin torque field is present.

Since, the material parameters are similar to the Co/Pt multilayer material and high DW velocities have been observed,⁴⁶ one might expect to measure also high β values. The results from the depinning field measurements are shown in Fig. 4.

The Oersted field contribution is zero within the error bars, whilst a non-zero contribution from spin torque effects exists at high current densities ($> 1 \times 10^{12}$ A/m 2). Compared to the spin torque contribution of the Co/Pt measurements, here a step-like dependence is observed with a threshold current density of about 1.5×10^{12} A/m 2 . This threshold current density and the fact that there is no linear dependence of the spin torque generated effective field on the current density point to the adiabatic torque as the driving mechanism and to $\beta \approx 0$. Measurements performed and published by other groups^{7,9} reveal a similar behavior, which is also explained by a dominant adiabatic spin torque requiring a critical current density to move the DW. The observed critical current density is of the same order of magnitude as in our present measurement.

D. Experimental results: Thermally activated domain wall motion in Co/Pt multilayer wires

To further investigate the non-adiabaticity factor β at 300 K, we now study the thermally activated DW motion under the influence of external fields and small injected DC

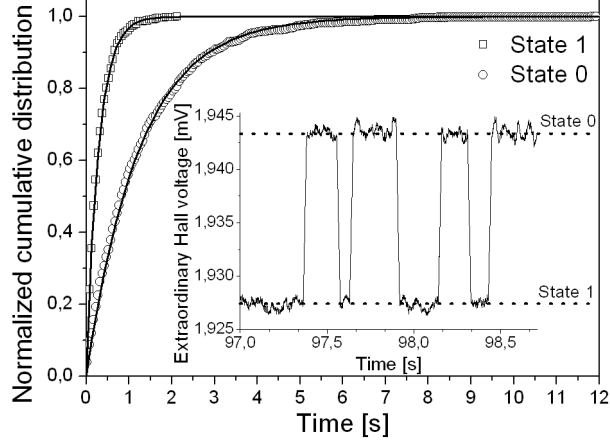


FIG. 5. The normalized cumulative distribution of both metastable states is fitted using the cumulative distribution function $F(t) = 1 - e^{-\frac{t}{\tau_S}}$ to extract the dwell time τ_S of state S (solid lines). The inset shows the time resolved extraordinary Hall voltage revealing two metastable states for a constant field (3.41 G) and a constant current $|I| = 0.5 \text{ mA}$, which corresponds to a current density of $J = 1.16 \times 10^{11} \text{ A/m}^2$.

currents, which cause no significant Joule heating effects. The low current densities ($< 1.2 \times 10^{11} \text{ A/m}^2$) used are also expected to be too small to significantly affect the shape of the DW. Using similar Co/Pt Hall cross structures we are able to measure the extraordinary Hall voltage in a time-resolved manner and to detect two metastable states (see Fig. 5(inset)). Thermal activation keeps the DW moving back and forth between the two states. As theoretically predicted, we observe a strong influence of the applied DC current or the applied field on the dwell times for which the DW remains in the states. We record the signal for several minutes before changing the current and/or applied field to obtain sufficient statistics of the dwell times. The error of each dwell time is hereby defined as the standard deviation of the mean value. For the case of constant currents (constant fields), we can see that the $\ln(\tau_1/\tau_0)$ scales linearly with the applied fields (applied DC currents).

1. *Current-field equivalence*

Fig. 6a shows the $\ln(\frac{\tau}{\tau_0})$ as a function of the applied field. It is shown that the reversal of the current polarity results in a translation of the values by a magnetic field ΔH using a fitted constant slope. This suggests that the injected current acts as an effective magnetic field.

Again, we can use the current-field equivalence approach ($\epsilon = \left| \frac{\Delta H}{\Delta J} \right| = \frac{\beta P \hbar}{2eM_S \lambda}$) to deduce β . For the various combinations of ΔH and ΔJ and considering their errors as weighing factors, we obtain an average value $\beta_{\text{effective}} = 0.13 \pm 0.02$. Repeating the experiment at a slightly lower temperature ($T \approx 287$ K) and using different metastable pinning states, we obtain β values ranging between 0.13 and 0.23 in line with the values obtained from the current-field equivalence in depinning field measurements mentioned in section III.B.1.

2. Arrhenius law approach

Next, we analyze the hopping measurements at constant fields. In Fig. 6b the $\ln(\frac{\tau}{\tau_0})$ is plotted as a function of the applied DC current: Here, we obtain values for β by following the Arrhenius approach. In order to do so, we analyze the current dependent shift in energy and use Eq. 8 to derive $\beta_{\text{Arrhenius}}$. The critical parameters, DW cross-sectional area $A = 4300 \text{ nm}^2$ and hopping distance $X_0 = 14.5 \text{ nm}$, can be approximated using the total change in extraordinary Hall voltage and the known width and thickness of the wire. From the measurements at different constant fields average values $\beta_{\text{Arrhenius}} = 0.013 \pm 0.001$ at $T \approx 296.6 \text{ K}$ and $\beta = 0.028$ at $T \approx 287.2 \text{ K}$ can be extracted, which turn out to be one order of magnitude smaller than the $\beta_{\text{effective}}$.

IV. CONCLUSIONS

In conclusion, we study Co/Pt and Co/Ni multilayer materials with a strong perpendicular uniaxial anisotropy to analyze the spin torque non-adiabaticity. Experimentally it is shown that we are able to separate the contributions to the DW depinning field and show that the Oersted field effect is negligibly small compared to the spin torque effects. We are also able to rule out the Joule heating effect causing a sample temperature increase. Nevertheless, for different Co/Pt sample structures we find consistent β values by following the current-field equivalence approach, thus showing that the high spin torque efficiency is intrinsic to the material and not stemming from other spurious effects. In case of the Co/Ni multilayer material, we extract a spin torque contribution, which is consistent with the adiabatic spin torque. An existing non-adiabatic spin torque contribution would have to be much smaller as shown in our measurements. A discrepancy arises during the study

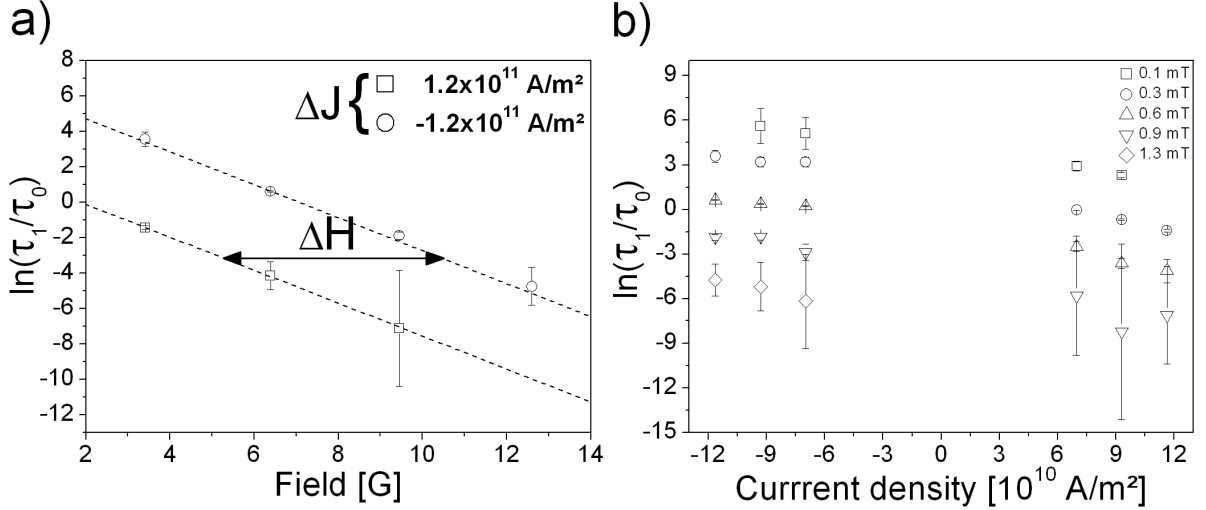


FIG. 6. a) $\ln(\frac{\tau_1}{\tau_0})$ as a function of the applied field for constant currents. For each value of a current we determine the slope by a linear fit weighed with errors of the individual measurements. The values of a current are then refitted using their average slope. b) $\ln(\frac{\tau_1}{\tau_0})$ as a function of the injected current density for different constant fields. The non-adiabaticity factor β is calculated from average slope of all fits.

of thermally activated DW motion on Co/Pt multilayer structures when analyzing the data of thermally activated DW motion experiments by using the Arrhenius law approach, which reveals a β value that is an order of magnitude smaller than the one deduced by the current-field approach. The entered parameters, cross-sectional area A and hopping distance X_0 necessary to solve Eq. 8 are calculated assuming a rigid and straight DW structure. This assumption necessary for a definition of X_0 and A might not hold for a DW entering a Hall cross with pinning sites. Deformations of a DW previously have been observed and a change of dimensionality has been shown by Kim et al.⁴⁷ Magnetic imaging techniques revealed here a transition from 1D- to 2D-behavior in the scaling criticality of creep DW motion as a function of the wire width. Related to the hopping distance, the activation volume is shown not to be proportional to the wire width in the 2D regime anymore. A more accurate determination can in our case be achieved by examining the hopping distance via time resolved magnetic imaging to measure X_0 and A . To compare to theory, full micromagnetic simulations at finite temperatures similar to Garcia-Sanchez et al.⁴⁸ are necessary, where it is shown that the effective deduced activation volume can be smaller than that assumed from the hopping distance in the 1D model. Therefore, a large uncertainty of the displacement

distance X_0 and cross-sectional area A might be present in our experiment highlighting the problems when analysing 2D-dynamics with 1D-models, while the current-field equivalence approach might prove more robust as it does not rely on these details.

V. ACKNOWLEDGMENTS

The authors would like to acknowledge the financial support by the DFG (SFB 767, KL1811), the Landesstiftung Baden Württemberg, the European Research Council via its Starting Independent Researcher Grant (Grant No. ERC- 2007-Stg 208162) scheme, EU RTN SPIN SWITCH (MRTN- CT-2006035327), the EU STREP project MAGWIRE (FP7- ICT-2009-5 257707), the Swiss National Science Foundation and the Samsung Advanced Institute of Technology.

REFERENCES

- ¹I. McFadyen, E. Fullerton, and M. Carey, MRS Bulletin **31**, 379 (2006).
- ²S. S. P. Parkin, M. Hayashi, and L. Thomas, Science **320**, 190 (2008).
- ³R. Cowburn, D. Petit, D. Read, and O. Petracic, Patent wo 2007/132174a1(2007).
- ⁴P. Xu, K. Xia, C. Gu, L. Tang, H. Yang, and J. Li, Nature Nanotechnology **3**, 97 (2008).
- ⁵P. Pavan, R. Bez, P. Olivo, and B. Zanoni, Proceedings of the IEEE **85**, 1248 (1997).
- ⁶D. Ilgaz, M. Klaui, L. Heyne, O. Boulle, F. Zinser, S. Krzyk, M. Fonin, U. Rudiger, D. Backes, and L. J. Heyderman, Appl. Phys. Lett. **93**, 132503 (2008).
- ⁷K. Ueda, D. Chiba, T. Koyama, G. Yamada, H. Tanigawa, S. Fukami, T. Suzuki, N. Ohshima, N. Ishiwata, Y. Nakatani, and T. Ono, Journal of Physics: Conference Series **266**, 012110 (2011).
- ⁸T. Koyama, G. Yamada, H. Tanigawa, S. Kasai, N. Ohshima, S. Fukami, N. Ishiwata, Y. Nakatani, and T. Ono, Applied Physics Express **1**, 101303 (2008).
- ⁹T. Koyama, D. Chiba, K. Ueda, K. Kondou, H. Tanigawa, S. Fukami, T. Suzuki, N. Ohshima, N. Ishiwata, Y. Nakatani, K. Kobayashi, and T. Ono, Nature Materials **10**, 194 (2011).
- ¹⁰H. Tanigawa, T. Koyama, G. Yamada, D. Chiba, S. Kasai, S. Fukami, T. Suzuki, N. Ohshima, N. Ishiwata, Y. Nakatani, and T. Ono, Applied Physics Express **2**, 053002

- (2009).
- ¹¹O. Boulle, L. Heyne, J. Rhensius, M. Kläui, U. Rüdiger, L. Joly, L. Le Guyader, F. Nolting, L. J. Heyderman, G. Malinowski, H. J. M. Swagten, B. Koopmans, C. Ulysse, and G. Faini, *Journal of Applied Physics* **105**, 07C106 (2009).
- ¹²L. Berger, *Journal of Applied Physics* **49**, 2156 (1978).
- ¹³J. Xiao, A. Zangwill, and M. D. Stiles, *Physical Review B* **73**, 054428 (2006).
- ¹⁴G. Tatara and H. Kohno, *Physical Review Letters* **92**, 086601 (2004).
- ¹⁵S. Zhang and Z. Li, *Physical Review Letters* **93**, 127204 (2004).
- ¹⁶A. Thiaville, Y. Nakatani, J. Miltat, and Y. Suzuki, *Europhysics Letters* **69**, 990 (2005).
- ¹⁷G. Tatara, T. Takayama, H. Kohno, J. Shibata, Y. Nakatani, and H. Fukuyama, *Journal of the Physical Society of Japan* **75**, 064708 (2006).
- ¹⁸A. Vanhaverbeke and M. Viret, *Physical Review B* **75**, 024411 (2007).
- ¹⁹X. Waintal and M. Viret, *Europhysics Letters* **65**, 427 (2004).
- ²⁰G. Tatara, H. Kohno, and J. Shibata, *Journal of the Physical Society of Japan* **77**, 031003 (2008).
- ²¹A. Thiaville, *Journal of Applied Physics* **95**, 7049 (2004).
- ²²D. G. Porter, *Journal of Applied Physics* **95**, 6729 (2004).
- ²³R. A. Duine, A. S. Núñez, and A. H. MacDonald, *Physical Review Letters* **98**, 056605 (2007).
- ²⁴O. Boulle, J. Kimling, P. Warnicke, M. Kläui, U. Rüdiger, G. Malinowski, H. J. M. Swagten, B. Koopmans, C. Ulysse, and G. Faini, *Physical Review Letters* **101**, 216601 (2008).
- ²⁵M. Viret, A. Vanhaverbeke, F. Ott, and J.-F. Jacquinot, *Physical Review B* **72**, 140403 (2005).
- ²⁶P. Hänggi, P. Talkner, and M. Borkovec, *Reviews of Modern Physics* **62**, 251 (1990).
- ²⁷J. P. Attané, D. Ravelosona, A. Marty, Y. Samson, and C. Chappert, *Physical Review Letters* **96**, 147204 (2006).
- ²⁸M. Eltschka, M. Wötzel, J. Rhensius, S. Krzyk, U. Nowak, M. Kläui, T. Kasama, R. E. Dunin-Borkowski, L. J. Heyderman, H. J. van Driel, and R. A. Duine, *Physical Review Letters* **105**, 056601 (2010).
- ²⁹C. Burrowes, A. P. Mihai, D. Ravelosona, J. Kim, C. Chappert, L. Vila, A. Marty, Y. Samson, F. Garcia-Sanchez, L. D. Buda-Prejbeanu, I. Tudosa, E. E. Fullerton, and J. Attané,

- Nature Physics **6**, 17 (2010).
- ³⁰C.-Y. You, I. M. Sung, and B.-K. Joe, Applied Physics Letters **89**, 222513 (2006).
- ³¹C.-Y. You and S.-S. Ha, Applied Physics Letters **91**, 022507 (2007).
- ³²S. Jung, W. Kim, T. Lee, K. Lee, and H. Lee, Applied Physics Letters **92**, 202508 (2008).
- ³³A. Mougin, M. Cormier, J. P. Adam, P. J. Metaxas, and J. Ferré, Europhysics Letters **78**, 57007 (2007).
- ³⁴P. J. Metaxas, J. P. Jamet, A. Mougin, M. Cormier, J. Ferré, V. Baltz, B. Rodmacq, B. Dieny, and R. L. Stamps, Physical Review Letters **99**, 217208 (2007).
- ³⁵D. Backes, C. Schieback, M. Kläui, F. Junginger, H. Ehrke, P. Nielaba, U. Rüdiger, L. J. Heyderman, C. S. Chen, T. Kasama, R. E. Dunin-Borkowski, C. A. F. Vaz, and J. A. C. Bland, Applied Physics Letters **91**, 112502 (2007).
- ³⁶J. Heinen, O. Boulle, K. Rousseau, G. Malinowski, M. Kläui, H. J. M. Swagten, B. Koopmans, C. Ulysse, and G. Faini, Applied Physics Letters **96**, 202510 (2010).
- ³⁷D. Ravelosona, S. Mangin, J. A. Katine, E. E. Fullerton, and B. D. Terris, Applied Physics Letters **90**, 072508 (2007).
- ³⁸S. Fukami, T. Suzuki, N. Ohshima, K. Nagahara, and N. Ishiwata, Journal of Applied Physics **103**, 07E718 (2008).
- ³⁹G. Meier, M. Bolte, R. Eiselt, B. Krüger, D. Kim, and P. Fischer, Physical Review Letters **98**, 187202 (2007).
- ⁴⁰L. Thomas, M. Hayashi, X. Jiang, R. Moriya, C. Rettner, and S. S. P. Parkin, Nature Physics **443**, 197 (2006).
- ⁴¹I. M. Miron, P.-J. Zermatten, G. Gaudin, S. Auffret, B. Rodmacq, and A. Schuhl, Physical Review Letters **102**, 137202 (2009).
- ⁴²L. San Emeterio Alvarez, K.-Y. Wang, S. Lepadatu, S. Landi, S. J. Bending, and C. H. Marrows, Physical Review Letters **104**, 137205 (2010).
- ⁴³L. Heyne, J. Rhensius, D. Ilgaz, A. Bisig, U. Rüdiger, M. Kläui, L. Joly, F. Nolting, L. J. Heyderman, J. U. Thiele, and F. Kronast, Physical Review Letters **105**, 187203 (2010).
- ⁴⁴A. Bisig, L. Heyne, O. Boulle, and M. Kläui, Applied Physics Letters **95**, 162504 (2009).
- ⁴⁵A. Barman, S. Wang, O. Hellwig, A. Berger, E. E. Fullerton, and H. Schmidt, Journal of Applied Physics **101**, 09D102 (2007).
- ⁴⁶T. Koyama, D. Chiba, K. Ueda, H. Tanigawa, S. Fukami, T. Suzuki, N. Ohshima, N. Ishiwata, Y. Nakatani, and T. Ono, Applied Physics Letters **98**, 192509 (2011).

⁴⁷K.-J. Kim, J.-C. Lee, S.-M. Ahn, K.-S. Lee, C.-W. Lee, Y. J. Cho, S. Seo, K.-H. Shin, S.-B. Choe, and H.-W. Lee, *Nature* **458**, 740 (2009).

⁴⁸F. Garcia-Sanchez, H. Szabolcs, A. P. Mihai, L. Vila, A. Marty, J.-P. Attané, J.-C. Toussaint, and L. D. Buda-Prejbeanu, *Physical Review B* **81**, 134408 (2010).